This expression is used to calculate the ratio for N-type silicon with resistivities 11.1 ohm-cm and 3.1 ohm-cm. In computing $|\kappa|$, it is recalled that ϵ_0 was defined by

$$\epsilon_0 = \epsilon_s + i\frac{\sigma_0}{\omega}$$

where $\epsilon_s = \epsilon_r\epsilon_v$ and ϵ_v is the permittivity of vacuum. At room temperature σ_0 reduces to σ_{dc}. Thus,

$$\kappa^2 = \omega^2\mu_0\epsilon_0 - k^2$$

leads to

$$|\kappa| = \frac{2\pi}{\lambda_0}\left\{[1 - (\lambda_0/\lambda_c)^2]^2 + [\sigma_{dc}/\omega\epsilon_s]^2\right\}^{1/4}$$

where $2\pi/\lambda_0 = \omega\sqrt{\mu_0\epsilon_s}$ and $\lambda_c = 2\pi/k$.

The following numerical values were used in the calculation:

$\epsilon_r = 12$ $\quad f = 22.235$ Gc/s

$\mu_H = 1450$ cm^2/volt-s $\quad \lambda_0 = 0.388$ cm

$B = 10$ kilogauss $\quad \lambda_c = 2.14$ cm

$y_0 = 0.43$ cm.

The resulting values for the ratio are

$R = 0.288$ for 11.1 ohm-cm

$R = 0.709$ for 3.1 ohm-cm.

Calculations on the basis of a model using the Boltzmann transport equation [10] lead to results which are smaller than the above values by a factor of 0.88 or 1.1 dB.

References

[1] G. J. Gabriel and M. E. Brodwin, "The solution of guided waves in inhomogeneous anisotropic media by perturbation and variational methods," *IEEE Trans. on Microwave Theory and Techniques*, vol. MTT-13, pp. 364–370, May 1965.

[2] B. Lax and L. M. Roth, "Propagation and plasma oscillations in semiconductors with magnetic fields," *Phys. Rev.*, vol. 98, pp. 548–549, 1955.

[3] G. J. Gabriel and M. E. Brodwin, "Distinctions between gyroelectric and gyromagnetic media in rectangular waveguide," this issue, page 292.

[4] P. H. Vartanian and E. T. Jaynes, "Propagation in ferrite-filled transversely magnetized waveguide," *IRE Trans. on Microwave Theory and Techniques*, vol. MTT-4, pp. 140–143, July 1956.

[5] B. Lax and K. J. Button, *Microwave Ferrites and Ferrimagnetics*. New York: McGraw-Hill, 1962, ch. 9, p. 355.

[6] A. D. Bresler, G. H. Joshi, and N. Marcuvitz, "Orthogonality properties for modes in passive and active uniform waveguides," *J. Appl. Phys.*, vol. 29, pp. 794–799, May 1958.

[7] G. J. Gabriel, Ph.D. dissertation, Northwestern University, Evanston, Ill., August 1964.

[8] R. E. Collin, *Field Theory of Guided Waves*. New York: McGraw-Hill, 1960, ch. 5, p. 170.

[9] J. K. Furdyna and S. Broesma, "Microwave Faraday effect in silicon and germanium," *Phys. Rev.*, vol. 120, pp. 1995–2003, December 1960.

[10] T. Burgess, Ph.D. dissertation, Northwestern University, Evanston, Ill., June 1965.

Log-Periodic Transmission Line Circuits—Part I: One-Port Circuits

R. H. DuHAMEL, FELLOW, IEEE, AND M. E. ARMSTRONG, MEMBER, IEEE

Abstract—A theoretical study of one-port log-periodic circuits consisting of a transmission line shunt loaded with open-circuit transmission lines is reported. The objective was to determine the conditions under which the phase of the input reflection coefficient varies linearly with the logarithm of the frequency. Precise definitions and general analytical techniques for log-periodic circuits are given. Results of extensive numerical calculations are presented to illustrate the dependence of the input reflection coefficient on the various design parameters. It was found that phase deviations from linear on the order of one degree are quite easily achieved.

Manuscript received October 21, 1965; revised February 17, 1966.

The authors are with the Hughes Aircraft Company, Ground Systems Group, Fullerton, Calif.

I. Introduction

THE OBJECTIVES here are to introduce and explain new concepts for transmission line circuits which are constructed according to log-periodic design principles. As with the corresponding log-periodic antennas, these circuits provide essentially frequency-independent performance over any desired finite bandwidth. Figure 1 illustrates strip line versions of the four types of circuits to be discussed. The lines in the drawings represent strips which may be inserted between parallel ground planes. The one-port circuit of Fig. 1(a), which is the subject of this report, can be de-

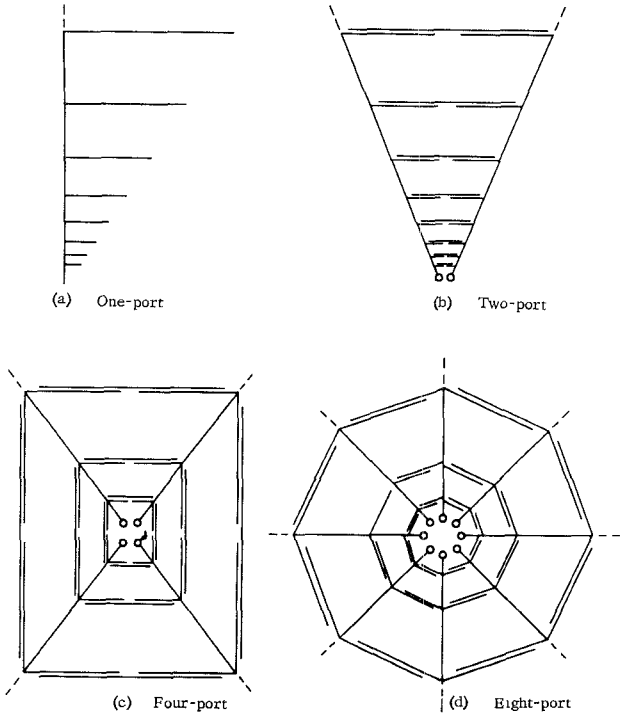

Fig. 1. Log-periodic transmission line circuits.

signed, such that the magnitude of the input reflection coefficient is constant and the phase varies linearly with the logarithm of the frequency.

As will be described in subsequent papers, the multiport circuits of Figs. 1(b), (c), and (d) may be designed to perform as matched junctions with certain desirable characteristics. Under certain conditions, the two-port circuit of Fig. 1(b) may be adjusted such that the phase of the transmission coefficient varies linearly with the logarithm of the frequency. A constant phase difference circuit may be achieved by using two identical two-port circuits, with the exception that one is scaled by a certain fraction of a period with respect to the other. The four-port circuit of Fig. 1(c) with two-fold symmetry can be designed to perform as a quadrature hybrid for which the coupled outputs are 90 degrees out of phase. The eight-port circuit of Fig. 1(d) with 45 degree rotational symmetry can function as a magic-T if opposite ports are connected as balanced pairs. By symmetry, there is isolation between orthogonal pairs of terminals and the coupled outputs are either in phase or out of phase.

Strictly speaking, these log-periodic circuits do not give frequency-independent performance, since the phase of the scattering coefficients varies, in general, in a log-periodic manner and, ideally, linearly with the logarithm of the frequency. However, the magnitudes of the scattering coefficients are essentially independent of frequency. This basic dispersive property of log-periodic structures was first observed by DuHamel and Ore [1] and was termed the phase rotation principle for log-periodic antennas. The significance of this dispersion on broadband signals was pointed out by Pulfer [2].

Considerable effort has been expended on the analysis of various log-periodic circuits and antennas. The most important is the classical work of Carrel [3] on the log-periodic dipole antenna. Using an equivalent circuit approach, he obtained complete solutions and design information for the antenna. DuHamel [4] discussed lumped-constant and distributed constant log-periodic circuits and derived exact solutions in terms of elliptic functions for a Foster type circuit consisting of an infinite number of series RLC networks connected in parallel. Mittra [5] extended the work of DuHamel and also analyzed a log-periodic lump-loaded transmission line. Precise definitions and the general characteristics of frequency-independent transmission lines and log-periodic circuits and transmission lines were given by DuHamel [6]. It was deduced that the input impedance of a log-periodic structure is a doubly periodic function of the logarithm of the complex frequency. An approximate solution for a lossless transmission line with log-periodic sinusoidal impedance variation was also given. Mittra and Jones [7] performed studies of the voltage distribution on frequency-independent (or continuously scaled) and log-periodic transmission lines shunt loaded with series RLC impedances. Since their objective was to gain a better understanding of the operation of antennas, such as the log-periodic dipole array, they concentrated on transmission lines for which the VSWR was small. Bevensee [8] derived variational expressions for the input impedance of lossless log-periodic transmission lines and classified them by their low-frequency behavior.

The log-periodic multiport circuits are based upon quite different design approaches. The design procedure may be summarized as follows.

1) The circuit is constructed so that its performance will be periodic with respect to the logarithm of the frequency.
2) Basic symmetries of the junction are specified so that the normal modes or eigenvectors are independent of frequency, and the eigenvalues allow the elements of the scattering matrix to assume the desired characteristics. The analysis of the circuit usually reduces, then, to the analysis of an equivalent single transmission line which is shunt and/or series loaded in a log-periodic manner.
3) If possible, the design parameters of the circuit are chosen so that the eigenvalue phases (or the input reflection coefficients of the normal modes) are linear functions of the logarithm of the frequency. This condition yields constant phase differences between eigenvalues, and hence the magnitudes of the elements of the scattering matrix will be independent of frequency.

4) Also, if practical, the design parameters are chosen so that the phase differences approximate particular values which, when achieved, cause certain elements in the scattering matrix of the circuit to vanish.
5) The number of cascades in the circuit is determined by the required bandwidth. To increase the bandwidth, it is only necessary to add on additional coupling sections. The largest dimension of the circuit is determined by the lowest frequency of operation. The high-frequency limit is determined by the length of the shortest coupling elements.

From the preceding procedures, it is apparent that the successful performance of log-periodic circuits depends critically upon achieving and controlling a linear phase characteristic for a transmission line loaded in a log-periodic manner. The objectives of this paper are to provide a physical insight into the behavior of simple one-port log-periodic transmission line circuits and to present the results of extensive computer investigations. Although emphasis is placed upon low-loss circuits, some interesting results are presented for circuits composed of low-Q transmission lines. Before discussing the numerical results, the definition, general characteristics and analytical procedures for log-periodic transmission line circuits are presented.

II. Theory and Analysis

A. Definition of Log-Periodic Circuits

The circuits to be considered in this paper consist of an infinite number of two-port networks connected in cascade as illustrated in Fig. 2, wherein reference directions for the voltage and current are defined. The voltage and current at terminals 1 of the nth network may be related to the voltage and current at terminals 1 of the $(n+1)$ network by the familiar $ABCD$ matrix,

$$\begin{vmatrix} V_n \\ I_n \end{vmatrix} = \begin{vmatrix} A_n & B_n \\ C_n & D_n \end{vmatrix} \times \begin{vmatrix} V_{n+1} \\ I_{n+1} \end{vmatrix} \tag{1}$$

where the subscripts 1 and 2 have been omitted. This cascaded network is defined to be log-periodic if the voltage and current satisfy the following functional equations:

$$\begin{aligned} V_n(p) &= V_{n+1}(\tau p) \\ I_n(p) &= I_{n+1}(\tau p) \end{aligned} \tag{2}$$

where p is the normalized complex angular frequency and the design ratio τ is a positive constant less than one. These simply state that the voltage and current at position n and frequency p are identical to those at position $n+1$ and frequency τp. The functional equations (2) are equivalent to first-order partial difference equations. The general solution for the voltage is given by [6]

$$V_n(p) = \tilde{f}(\ln p)\Phi(\tau^{-n}p) \tag{3}$$

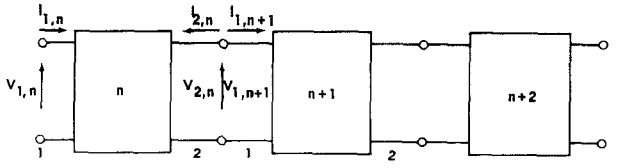

Fig. 2. Cascade of two-port circuits.

where f is an arbitrary periodic function with period $|\ln \tau|$ and Φ is an arbitrary function. Arbitrary periodic functions always arise in the solution of difference equations with a continuous independent variable. For a particular problem they may be determined from the boundary conditions [9]. The general solution for the current is the same form as (3).

In order to determine the restrictions that (2) place on the elements of the $ABCD$ matrix, rewrite (1) in terms of the independent variables $n+1$ and τp and compare the new equations with (1). It is then found that the matrix elements must satisfy functional equations identical to (2); i.e.,

$$A_n(p) = A_{n+1}(\tau p), \quad \text{etc.}$$

The general solution for the matrix elements may be written as

$$A_n(p) = \Phi(\tau^{-n}p). \tag{4}$$

The arbitrary periodic function has been omitted since this type of frequency variation is impractical to achieve.

If voltage and current generator terms were included in (1), it would be found that the solutions for the sources would also be of the form (4). If it is specified that there be only one shunt current generator J in the cascade, an allowable solution is

$$\begin{aligned} J_n(p) = \Phi(\tau^{-n}p) &= 1, \qquad \tau k < \tau^{-n}p \leq k \\ &= 0, \qquad \tau^{-n}p \leq \tau k \leq \tau^{-n-1}p \end{aligned} \tag{5}$$

where k is a constant. This type of source must move from one terminal pair of the cascade to an adjacent pair when the frequency is changed by τ (or a period). If k approaches zero, then the source will appear infinitely far to the left in Fig. 2. We will be interested only in circuits for which the elements of the $ABCD$ matrix assume the limiting forms

$$\begin{aligned} \lim_{n\to-\infty} A_n &= \lim_{n\to-\infty} D_n = 1 \\ \lim_{n\to-\infty} B_n &= \lim_{n\to-\infty} C_n = 0. \end{aligned} \tag{6}$$

These relations imply that the network becomes a transmission line of infinitesimal length as $n\to-\infty$. Thus if it is specified that $k\to 0$ in (5), the particular location of the source is immaterial if it is placed at a terminal pair such that the conditions (6) are closely approximated. In this sense then, the source may be considered as a fixed frequency-independent source.

Under the conditions (6) it is apparent that the volt-

age and current become independent of n as $n \to -\infty$. Thus, the voltage and current (and hence the impedance) are periodic functions of the logarithm of the frequency. Since the voltage and current must be single-valued functions of the complex frequency p, it may be immediately argued that they are doubly periodic functions of $\ln p$ and may be represented by elliptic functions. The equivalent mathematical statement is

$$\lim_{n \to -\infty} V_n(p) = \bar{f}(\ln p) = \bar{f}(\ln p + r \ln \tau + sj2\pi). \quad (7)$$

This simply states that the magnitude of p may be changed by the factor τ^r and the phase by $s2\pi$, where r and s are integers, without changing $\bar{f}$ or V. The real and imaginary periods of the doubly periodic function are $\ln \tau$ and 2π, respectively. Thus we have the important conclusion that doubly periodic functions should appear in the exact solutions for log-periodic structures. This has been verified for the simple case of an infinite number of series LC circuit elements placed in parallel [6].

The particular circuit which is the major subject of this report is illustrated in Fig. 3. The circuit may be considered as an infinite cascade of symmetrical cells consisting of transmission lines of length $\bar{\theta}_n$ and characteristic impedance Z_1 shunt loaded by open-circuit lines of length θ_n and impedance Z_2. The elements of the $ABCD$ matrix are, for the lossless case, given by

$$\begin{aligned} A_n &= D_n = \cos \bar{\theta}_n - \frac{Z_1 \sin \bar{\theta}_n}{2Z_2 \cot \theta_n} \\ B_n &= jZ_1 \left[\sin \bar{\theta}_n + \frac{Z_1(\cos \bar{\theta}_n - 1)}{2Z_2 \cot \theta_n} \right] \\ C_n &= \frac{j}{Z_1} \left[\sin \bar{\theta}_n + \frac{Z_1(\cos \bar{\theta}_n + 1)}{2Z_2 \cot \theta_n} \right]. \end{aligned} \quad (8)$$

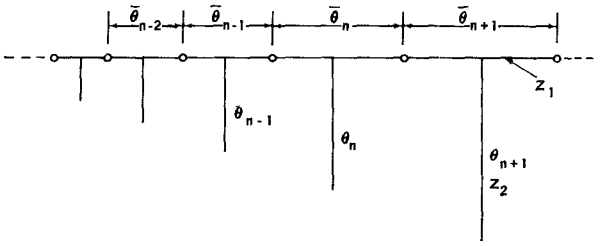

Fig. 3. Log-periodic shunt loaded transmission line.

If losses are to be included in the circuit, then $\bar{\theta}_n$ is replaced by $\bar{\theta}_n(1 - j/2Q)$ where $Q = \beta/2\alpha$. Adjacent section line lengths are related by

$$\tau = \frac{\theta_n}{\theta_{n+1}} = \frac{\bar{\theta}_n}{\bar{\theta}_{n+1}}. \quad (9)$$

By expressing the line lengths in terms of, say, the Nth section line length,

$$\theta_n = \tau^{N-n}\theta_N, \qquad \bar{\theta}_n = \tau^{N-n}\bar{\theta}_N \quad (10)$$

it is apparent that (8) satisfies (4), since θ_N is proportional to the frequency.

B. General Performance Characteristics

The infinite cascade of Fig. 3 may be divided into several regions. Near the input, the cell image impedance approaches a constant value given by

$$Z_0 = \lim_{n \to -\infty} \left| \frac{B_n}{C_n} \right|^{1/2} = Z_1 \left| 1 + \frac{\eta}{\sigma} \right|^{-1/2} \quad (11)$$

where $\sigma = \bar{\theta}_n/\theta_n$ and $\eta = Z_1/Z_2$. Hence, in this region, the structure is equivalent to a uniform transmission line. For some distance past the input region the image impedances of adjacent cells are only slightly different so that the structure is equivalent to a slowly varying nonuniform transmission line. Beyond this latter region, large changes in the cell image impedance occur, and eventually the cell image impedance and propagation function become complex. This is termed the stop or reflection region and occurs when the stub length is somewhat shorter than a quarter wavelength. Past this first stop region there are alternate pass and stop regions.

An incident wave applied at the input propagates along the structure and is partially or completely reflected at the first stop region. If complete reflection takes place, then ideally the input reflection coefficient is given by

$$\Gamma = \exp\left[-j \frac{2\pi \ln \theta_N}{|\ln \tau|} + \chi \right] \quad (12)$$

where θ_N is proportional to frequency and χ is a constant. The reflection coefficient has been normalized to (11). Note that the form of the reflection coefficient is similar to that of an open-circuited transmission line except that the argument of the exponential function is proportional to the logarithm of the frequency rather than frequency. Curve A of Fig. 4 illustrates this linear phase variation wherein the phase changes by 2π radians when the frequency is changed by the factor τ or a period. Calculations show that the phase of the reflection coefficient varies as curve B, wherein the phase deviates from the desired straight line characteristic by a maximum value denoted by Δ_M. For given values of σ, η, and Q, this phase characteristic is achieved for τ greater than some minimum value. Maximum phase deviations of several degrees are ordinary and deviations of only a small fraction of a degree are possible.

If complete reflection does not occur at the first stop region, then a portion of the wave propagates to the next stop region where it is partially or completely reflected. This leads to large phase deviations from the desired linear characteristics and, in some cases, to jumps of 2π as illustrated by curve C.

If all dimensions of the circuit of Fig. 3 are scaled gradually from the original to τ times the original dimensions, it is easily shown that the phase curve moves

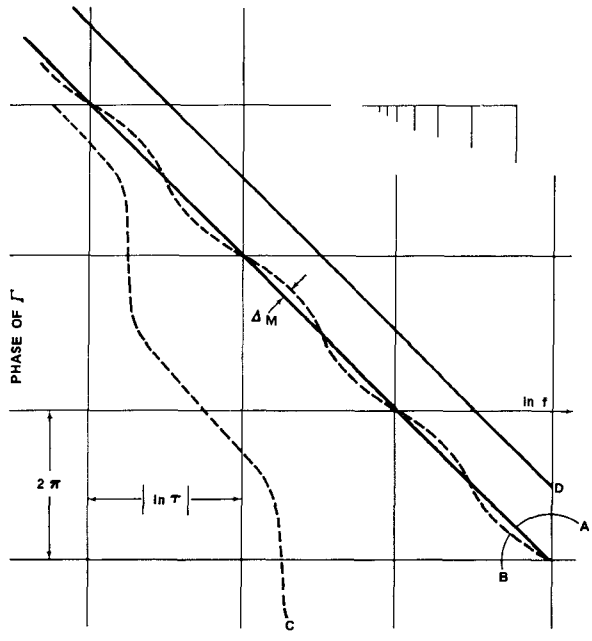

Fig. 4. Reflection coefficient phase characteristics of log-periodic circuits.

up by the amount 2π. A scaling of $\sqrt{\tau}$ with a phase change of π is illustrated by curve D of Fig. 4. This phenomena is analogous to the phase rotation principle for log-periodic antennas and is useful in the design of constant phase difference circuits.

C. Analytical Procedures

The log-periodic cascades may be solved by straightforward, but tedious, matrix multiplication. The numerical results described later were all obtained with the aid of a high-speed computer. It is desirable to have exact closed form solutions since this would greatly simplify the design of multiport circuits. However, this seems impossible for most cases considered. As an alternative, it is quite desirable to have approximate solutions which could provide approximate design procedures or, at the least, qualitative information. Several approaches to this end are described.

In general, the networks may be lossy. However, two limiting cases are of the most importance. The first is when the networks are lossless, in which case the input impedance of the structure is totally reactive and varies with frequency in a log-periodic manner. An approximate solution for this case would be quite helpful. In the second case, the loss is such that practically all of the incident energy is absorbed and the reflected wave is small or negligible. Approximate solutions for this case can be obtained by approaches analogous to the WKBJ method.

Equations (1) are simultaneous, first-order difference equations. A second-order difference equation in one dependent variable may be easily obtained by eliminating the other. The result is

$$V_{n+2} - V_{n+1}\left[\frac{A_n B_{n+1}}{B_n} + D_{n+1}\right] + V_n \frac{B_{n+1}}{B_n} = 0. \quad (13)$$

In principle, this second-order difference equation may be solved by techniques analogous to those used for second-order differential equations. However, since the variable coefficients have such complicated forms, it is usually impossible to obtain exact closed form solutions. For example, if the $ABCD$ elements given by (8) are substituted in (13) and use is made of (10), it will be found that the independent variable n appears as an exponent in the argument of the trigonometric functions. As $n \rightarrow -\infty$, the coefficients reduce to constants and the solution in this region is simple. However, this is of little use since it applies only in the region where the cascade is equivalent to a uniformly loaded transmission line. The problem may also be attacked from an impedance view. Let

$$Z_n = \frac{V_n}{I_n}. \quad (14)$$

Dividing the first equation of (1) by the second, and rearranging terms, a nonlinear first-order difference equation is obtained.

$$Z_n Z_{n+1} C_n - (Z_{n+1} - Z_n) A_n - B_n = 0. \quad (15)$$

It has been assumed that each cell is symmetrical such that $A_n = D_n$. In general, this equation is quite difficult to solve. A solution may be obtained for the special and somewhat trivial case where the image impedances of all the cells are identical; that is,

$$Z_{0,n} = \sqrt{\frac{B_n}{C_n}} = Z_0. \quad (16)$$

Under these conditions, the solution for the cascade may be written as [10]

$$Z_n = Z_0 \tanh\left[C + \sum_{n_0}^{n-1} \tanh^{-1} \frac{-C_n Z_0}{A_n}\right], \quad (17)$$

where n_0 is the starting point of the network (ideally $n_0 = -\infty$) and C is a constant.

In some cases a better physical insight to cascaded networks may be obtained by analyzing them in terms of incident and reflected waves rather than voltage and current. In the following the waves are related to the voltage and current by image impedances which are a function, in general, of n. Figure 5 illustrates a cascade of symmetrical two-port networks with image propagation functions ϕ_n and image impedances $Z_{0,n}$. These functions are given by

$$Z_{0,n} = \sqrt{\frac{B_n}{C_n}} \quad (18)$$

$$e^{\pm\phi_n} = A_n \pm \sqrt{B_n C_n}. \quad (19)$$

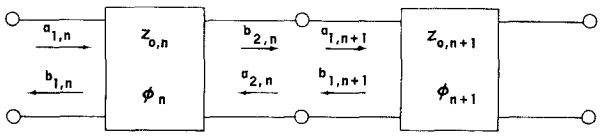

Fig. 5. Definition of wave functions for cascade.

The image impedances are defined such that, if the network is terminated in the image impedances, the propagation through the network is expressed by exponential ϕ_n. To show how this comes about, make the substitutions

$$V_{1,n} = Z_{0,n}^{1/2}[a_{1,n} + b_{1,n}],$$
$$V_{2,n} = Z_{0,n}^{1/2}[a_{2,n} + b_{2,n}] \tag{20}$$
$$I_{1,n} = Z_{0,n}^{-1/2}[a_{1,n} - b_{1,n}],$$
$$I_{2,n} = Z_{0,n}^{-1/2}[-a_{2n} + b_{2,n}] \tag{21}$$

into (1). This assumes, of course, that $Z_{0,n}$ is nonzero, which holds for most LP circuits only if losses are included. Rearranging, it is found that the a's and b's are related by

$$\begin{bmatrix} a_{1,n} \\ b_{1,n} \end{bmatrix} = \begin{bmatrix} e^{\phi_n} & 0 \\ 0 & e^{-\phi_n} \end{bmatrix} \times \begin{bmatrix} b_{2,n} \\ a_{2,n} \end{bmatrix}. \tag{22}$$

Referring to Fig. 5, what we desire is a wave matrix of the form

$$\begin{bmatrix} a_{1,n} \\ b_{1,n} \end{bmatrix} = \begin{bmatrix} A_{11,n} & A_{12,n} \\ A_{21,n} & A_{22,n} \end{bmatrix} \begin{bmatrix} a_{1,n+1} \\ b_{1,n+1} \end{bmatrix} \tag{23}$$

which relates the incident and reflected waves ($a_{1,n}$ and $b_{1,n}$, respectively) for adjacent networks. Since the image impedance of network n may be different from the image impedance of network $n+1$, care must be taken in satisfying the boundary conditions which are that the voltage and current are continuous. Then making use of the boundary conditions, it may be shown that the desired matrix relation is given by (omitting the subscripts 1 and 2)

$$\begin{bmatrix} a_n \\ b_n \end{bmatrix} = \xi_n \begin{bmatrix} e^{\phi_n} & \rho_n e^{\phi_n} \\ \rho_n e^{-\phi_n} & e^{-\phi_n} \end{bmatrix} \begin{bmatrix} a_{n+1} \\ b_{n+1} \end{bmatrix} \tag{24}$$

where

$$\rho_n = \frac{Z_{0,n+1} - Z_{0,n}}{Z_{0,n+1} + Z_{0,n}}$$

and

$$\xi_n = \frac{Z_{0,n+1} + Z_{0,n}}{2(Z_{0,n+1}Z_{0,n})^{1/2}}.$$

The quantity ρ_n is similar to a reflection coefficient and represents the mismatch between adjacent cells of the network. ξ_n is nearly equal to one except in the reflection region.

Figure 6(a) illustrates the variation of $Z_{0,n}$ and ϕ_n as a function of θ_n as determined from (8), (18), and (19) for a cell of the circuit of Fig. 3. The results are for a typical case of $Q=\infty$, $\eta=2$, and $\sigma=1$. Figure 6(b) shows the corresponding variation of $|\rho_n|$ and $|\xi_n|^{-1}$ for the case of $\tau=0.841$. It will be noticed that $|\rho_n|$ is quite small except in the reflection region where it takes on the value one over a bandwidth determined by τ. For finite Q, the discontinuities in the curves of Fig. 6(b) would not be present. As before, the performance of the complete network may be obtained by straightforward matrix multiplication.

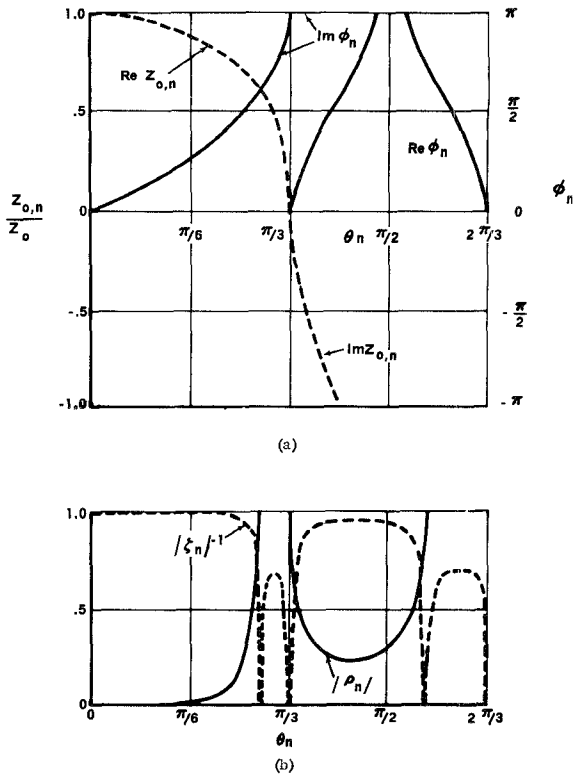

Fig. 6. Frequency dependence of image parameters for cell of circuit of Fig. 3.

This representation of the cascade network gives, in some cases, considerable insight into the performance of the network. For example, writing the first equation of (24) we have

$$a_n = \xi_n[e^{\phi_n}a_{n+1} + \rho_n e^{\phi_n}b_{n+1}]. \tag{25}$$

If there is loss in the circuit such that the reflected wave b_{n+1} is small, then the second term on the right may be neglected to give, approximately,

$$a_{n+1} = \frac{e^{-\phi_n}}{\xi_n} a_n. \tag{26}$$

The solution of this simple first-order difference equation is

$$a_n = \prod_{n_0}^{n-1} \frac{e^{-\phi_n}}{\xi_n} \tag{27}$$

which may be further simplified by assuming ξ_n equals one to give

$$V_n = \left[\frac{Z_{0,n}}{Z_{0,n_0}}\right]^{1/2} \prod_{n_0}^{n-1} e^{-\cosh^{-1} A_n} \tag{28}$$

where use has been made of (19) and (20). This solution for the cascaded networks is analogous to the WKBJ solution for a continuously varying transmission line. A similar solution can be obtained for b_n. These solutions would be expected to be accurate except in regions where ρ_n and ξ_n differ appreciably from zero and one, respectively.

The second-order difference equation for a_n, derived from (24), is

$$a_{n+2} - a_{n+1}\xi_{n+1}\left(e^{-\phi_{n+1}} + \frac{\rho_{n+1}}{\rho_n} e^{\phi_{n+1}}\right) + a_n \frac{\xi_{n+1}\rho_{n+1}}{\xi_n \rho_n} e^{\phi_{n+1}-\phi_n} = 0. \tag{29}$$

Again, it seems impossible to obtain closed form solutions because of the complexity of the coefficients for the circuits of interest.

Defining a pseudoreflection coefficient by

$$\Gamma_n = \frac{b_n}{a_n} \tag{30}$$

and dividing the second equation of (24) by the first, we obtain the nonlinear equation

$$\Gamma_{n+1}\Gamma_n \rho_n e^{\phi_n} - \Gamma_{n+1} e^{-\phi_n} + \Gamma_n e^{\phi_n} - \rho_n e^{-\phi_n} = 0. \tag{31}$$

If the reflection coefficient on the line is small, the first term may be neglected with respect to the others. The solution of the resulting first-order linear difference equation may be written as

$$\Gamma_n = \sum_{m=n}^{\infty} \rho_m \prod_{n}^{m} e^{-2\phi_n} \tag{32}$$

where Γ_n is the reflection coefficient looking into the nth section toward the right in Fig. 5. It is seen that this is simply the sum of reflections at the junctions of adjacent cells delayed by the proper propagation functions. From observation of Fig. 6, it is apparent that the reflection region is the major contributor to the magnitude of the input reflection coefficient. Attempts to obtain simple closed form solutions to (32) for the circuit of Fig. 3 have been unsuccessful.

D. Computational Procedure

Since attempts to obtain closed form solutions for LP networks were unsuccessful, it was necessary to resort to the use of a high-speed computer. Since knowledge of the input reflection coefficient of LP networks is sufficient to determine their performance, calculations of the internal voltages and currents were not performed. It is expected that the voltage distribution would be similar to that reported by Mittra and Jones [7].

Ideally, the circuit consists of an infinite number of cells. Since the calculation and construction of the ideal circuit is impossible, calculations were made for networks with a finite number of cells numbered from 1 to N. To account approximately for the deleted cells numbered from 0 to $-\infty$, a compensation transmission line section of length ψ_0 and characteristic impedance Z_0 was added to the network as illustrated in Fig. 7. The length is determined from

$$\psi_0 = \sum_{n=0}^{-\infty} \phi_n$$

or

$$\psi_0 \approx \phi_0 \sum_{n=0}^{-\infty} \tau^{-n} = \frac{\phi_0}{1-\tau} \tag{33}$$

provided ϕ_0 is small. Z_0 is determined from (11).

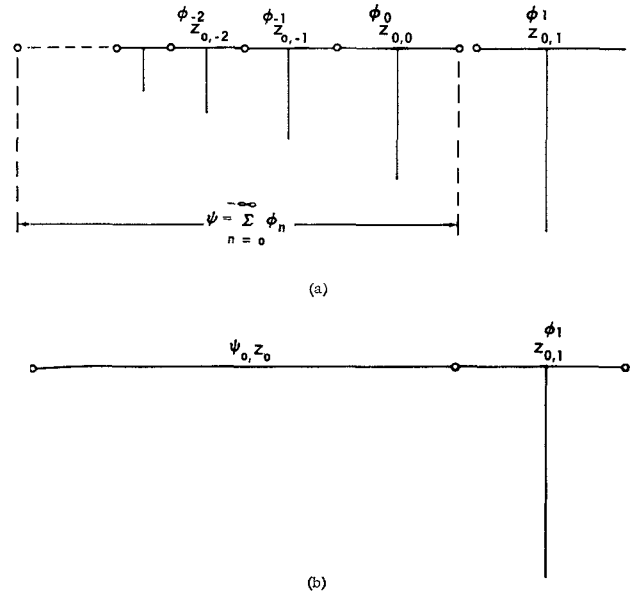

Fig. 7. Compensation section for log-periodic circuit.

The $ABCD$ matrix for the complete network may be obtained by straightforward matrix multiplication as follows:

$$\begin{vmatrix} A & B \\ C & D \end{vmatrix} = \prod_{n=0}^{N} \begin{vmatrix} A_n & B_n \\ C_n & D_n \end{vmatrix} \tag{34}$$

where

$$A_0 = \cos \psi_0$$
$$B_0 = jZ_0 \sin \psi_0$$
$$C_0 = \frac{j}{Z_0} \sin \psi_0$$
$$D_0 = \cos \psi_0$$

and the other matrix elements are determined from the cell configuration. The input reflection coefficient, normalized to Z_0, is then given by

$$\Gamma = \frac{AZ_{N+1} + B - Z_0(CZ_{N+1} + D)}{AZ_{N+1} + B + Z_0(CZ_{N+1} + D)} \tag{35}$$

where Z_{N+1} is the termination impedance placed on the output of cell N.

The input reflection coefficient was calculated m frequencies per period for several periods. The computer program was designed so that the magnitude and phase of the reflection coefficient were printed both graphically and numerically vs. the logarithm of the frequency. The deviation of the phase from linear was also printed graphically. This allowed a quick determination of the performance of the circuit.

The objective was to determine conditions on the circuit parameters so as to achieve a linear phase characteristic. Since it was found that there was negligible end effect for circuits with nearly linear phase variation, the termination impedance had negligible effect upon Γ except below the cutoff frequency. Most of the results were obtained with $Z_{N+1} = Z_0$.

III. Numerical Results

Although calculations have been performed for a wide variety of log-periodic transmission line circuits, the majority of results reported here are for the circuit of Fig. 3. The performance of most of the other circuits (see Part II—Two-Port Circuits) is quite similar.

The compensating section length ψ_0 is determined from

$$\psi_0 = \frac{\phi_0}{1-\tau} = \frac{\cos^{-1} A_0}{1-\tau} \approx \frac{\left(1 + \frac{\eta}{\sigma}\right)^{1/2} \theta_0}{1-\tau} \tag{36}$$

where A_0 is determined from (8) and it is assumed that θ_0 is small.

The circuit computations were originally made for lossless circuits (i.e., infinite Q). By making computations at a sufficient number of frequencies per period, it was nearly always found that phase jumps or end effect would occur in an extremely small bandwidth. Except at a frequency where a stub is $\lambda/4$, there is always a finite but extremely small coupling to the circuit structure beyond the reflection region. The phase jumps are due to resonance involving this coupling. By inserting a small loss in the circuit elements, these resonances may be damped out. Thus, it is important to use reasonable Q values in computer investigations of log-periodic circuits.

The phase deviation Δ for a ten-section transmission line circuit is plotted in Fig. 8 vs. the normalized frequency over a 20 to 1 bandwidth. Scales showing θ_N and θ_1 vs. frequency are also included. The spacing between vertical lines is equal to two periods of frequency. If we define the bandwidth of the circuit as the frequency range for which the phase deviation is less than five degrees, it is seen that the structure has a bandwidth of 11 to 1. The low- and high-frequency cutoffs occur when

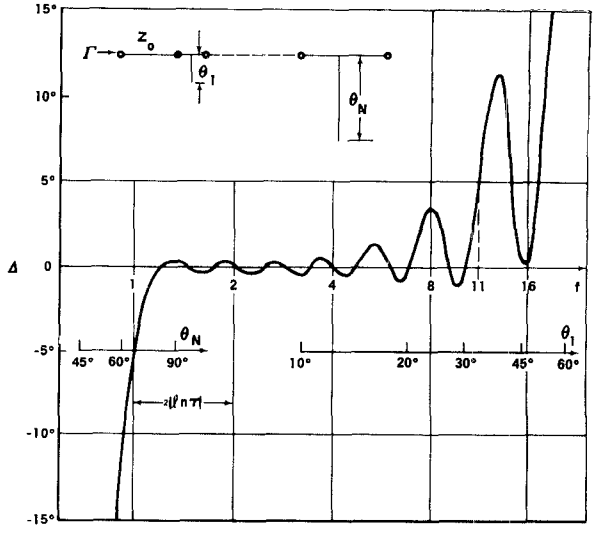

Fig. 8. Phase deviation from linear of log-periodic circuit.

θ_N and θ_1 are approximately 65° and 40°, respectively. The low-frequency cutoff occurs approximately when the propagation function ϕ_N becomes equal to π, i.e., at the onset of the stop band for cell N. From these results, the bandwidth of an N section circuit with the same parameters is readily inferred to be $0.48\tau^{-N+1}$.

For normalized frequencies from 1.3 to 3, it will be noticed that the maximum phase deviation from linear is approximately frequency-independent and is less than one degree. This performance would be expected over the complete spectrum for a truly log-periodic circuit with an infinite number of sections. For frequencies greater than 3, the maximum phase deviation increases rapidly. This is due to the mismatch between the compensation section and the first section of the circuit. A brief discussion of this is given in Section IV. If this compensation section were not included, then the phase deviation from linear would be much greater.

A portion of a large number of parameter investigations of the simple circuit of Fig. 3 is summarized in Figs. 9–12. The important design parameters are τ, σ, Q, and η. The curves show the variation of the maximum phase deviation and magnitude of the reflection coefficient vs. one of the above parameters. The common set of parameters for the four figures are:

$$\tau = 0.841, \qquad \sigma = 1, \qquad Q = 200, \qquad \eta = 2.$$

These values were chosen since they are similar to those used for practical multiport circuits.

Figure 9 illustrates the variation of the magnitude $|\Gamma|$ and maximum phase deviation from linear, Δ_M, of the input reflection coefficient vs. the design ratio τ. The empirical expression

$$|\Gamma| = \exp\left[\frac{-\pi}{Q|\log \tau|}\right] \tag{37}$$

was determined from a large number of computer results. Surprisingly, this formula is accurate to the third

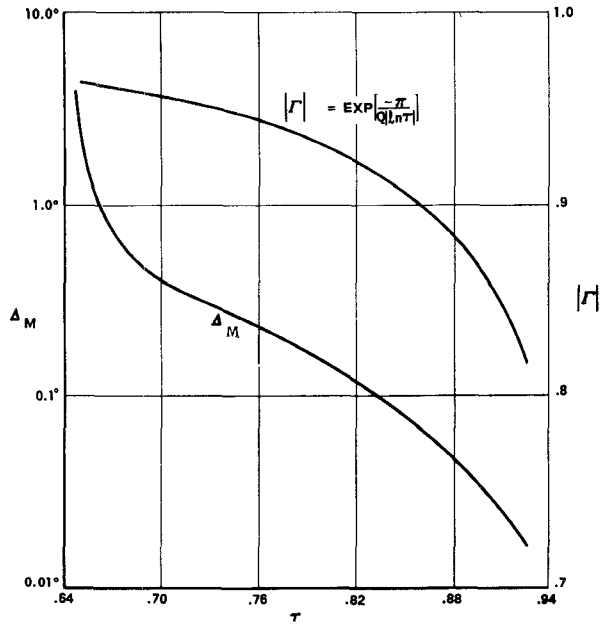

Fig. 9. Dependence of Δ_M and $|\Gamma|$ on τ. $\eta=2$, $\sigma=1$, $Q=200$.

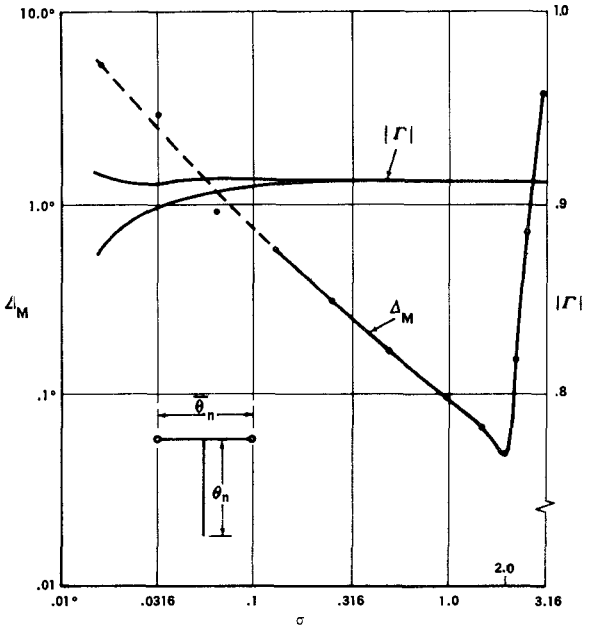

Fig. 11. Dependence of Δ_M and $|\Gamma|$ on σ. $\tau=0.841$, $\eta=2$, $Q=200$.

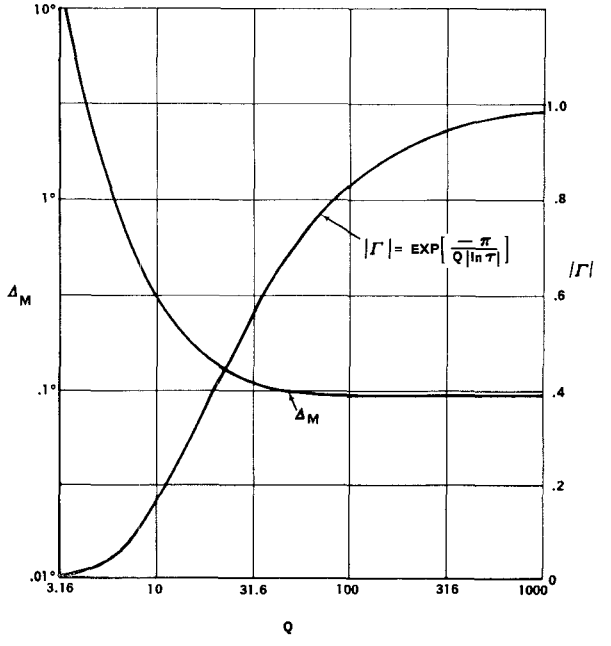

Fig. 10. Dependence of Δ_M and $|\Gamma|$ on Q. $\eta=2$, $\sigma=1$.

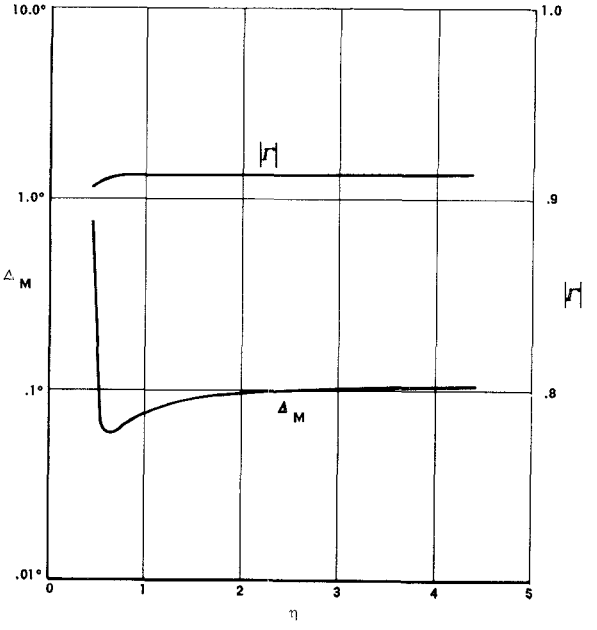

Fig. 12. Dependence of Δ_M and $|\Gamma|$ on η. $\tau=0.841$, $\sigma=1$, $Q=200$.

decimal point for an extremely wide range of Q and τ, provided the circuit has no end effect. Equally surprising, $|\Gamma|$ is essentially independent of σ and η. The magnitude of the reflection coefficient drops off quite rapidly as τ approaches one. This is to be expected since for a *lossless* circuit the ratio of the stored energy W to the incident power P is given by (Montgomery et al. [11])

$$\frac{W}{P} = j\frac{\Gamma^*}{2\pi}\frac{d\Gamma}{df} \tag{38}$$

where * denotes the complex conjugate. Substituting from (12) we have

$$\frac{W}{P} = \frac{1}{f|\log\tau|}. \tag{39}$$

Thus, as τ approaches one, the stored energy increases rapidly. Hence, for a lossy circuit it is expected that the dissipation would increase as the stored energy increases.

It will be noticed that Δ_M becomes quite large for τ less than 0.68. For τ less than 0.65, end effect and hence, rapid phase jumps, are encountered since the shunt stubs do not load the line heavily enough to cause complete reflection in the reflection region.

As τ is increased, Δ_M decreases rapidly to a value of

0.02 degree at τ equal to 0.92. This trend might also be expected since the bandwidth of a period decreases as τ increases. For these calculations it was necessary to make N large enough so that the phase deviations due to the "mismatch" of the compensation section were less than the phase deviations of the basic log-periodic circuit. For $\tau < 0.80$, 20 sections were used. For larger τ, N was increased such that the phase deviation due to the mismatch was less than 0.01 degree. For $\tau = 0.92$, this required 60 sections. The frequency range was chosen so that θ_N was always greater than 180 degrees.

For most applications it is desirable to have Δ_M small (on the order of one degree) and $|\Gamma|$ nearly equal to one. As can be seen from Fig. 9, a compromised value of τ must be chosen.

In Fig. 10, $|\Gamma|$ and Δ_M are shown as a function of Q. For Q greater than 30, Δ_M is practically independent of Q. Δ_M increases rapidly as Q is decreased below 30. For the lossy circuits, the input characteristic impedance will be complex rather than real as given by (3). If $|\Gamma|$ had been normalized to this complex impedance, it is likely that Δ_M would be much smaller for small Q. For typical strip line construction, Q is on the order of several hundred.

Since the magnitude of the reflection coefficient drops off quite rapidly as Q is decreased, it is apparent that low-loss transmission lines should be used for log-periodic circuits. The empirical formula is accurate even for $Q = 3.16$ where $|\Gamma| = 0.003$.

It is interesting to compare the performance of this transmission line circuit with simple log-periodic antennas such as the dipole array. The latter consists of a lossless transmission line shunt loaded with thin dipoles. The input impedance of a dipole is approximately given by that of a lossy open-circuited transmission line [12] with a length equal to half the dipole length. For typical dipoles, the Q of the equivalent transmission line is on the order of 5 to 10. Since $\tau = 0.841$ is reasonable for a log-periodic dipole antenna, it would be expected from the curve of Fig. 10 that the input reflection coefficient should be on the order of 0.1. This corresponds quite closely to reported measurements. (The reflection coefficient locus for an LP antenna is very similar to that for a LP circuit.) If attempts are made to reduce the size of a LP antenna by foreshortening the dipoles and hence increasing the Q of the dipoles it would be expected that the input reflection coefficient should rise rapidly. This phenomena has been observed by many workers in the field. The increase in $|\Gamma|$ might be counteracted by increasing τ. Of course, in an LP antenna, the effective Q of the dipole radiators depends in a complex manner on the mutual impedances and the design parameters. Thus, the above discussion should only be interpreted as qualitative.

Figure 11 illustrates the dependence of $|\Gamma|$ and Δ_M on σ. For extremely small σ, $|\Gamma|$ varies over a period of frequency. The two curves indicate the upper and lower bounds of $|\Gamma|$. It is quite surprising that $|\Gamma|$ is essentially independent of σ over an extremely wide range. For example, as σ varies from 0.1 to 2, the length of the transmission line (with impedance Z_1) from the feed point to the reflection region varies from 0.16 to 3.2 λ; yet the losses in the circuit do not change. Apparently, most of the loss takes place in the shunt stubs. The phase deviation from linear reaches a minimum of 0.05 degree at $\sigma = 2$. Thus, in the reflection region, a spacing between adjacent stubs of approximately $\lambda/2$ gives a minimum Δ_M. The maximum useable value of σ is about three, since for larger σ end-effect is observed.

The effect of η on the input reflection coefficient is shown in Fig. 12. Both $|\Gamma|$ and Δ_M are essentially independent of η for this ratio greater than one. For η less than 0.5, end-effect occurs.

It was hoped that simple empirical formulas or rules could be derived for the minimum design ratio τ_m to achieve no end-effect and a maximum phase deviation. However, it appears that τ_m is a very complicated function of η, σ, and Q. It is best to determine τ_m with the aid of a computer for each particular circuit. The approximate dependence of τ_m on η is given in Table I.

TABLE I

η	τ_m
1/2	0.88
1	0.80
2	0.68
4	0.58

The criteria for this table is that Δ_M be less than one degree.

IV. Phase Characteristics of the Reflection Coefficient

As discussed previously, it is desired that the input reflection coefficient of a lossless one-port log-periodic circuit be of the form $\Gamma = \exp[-j\gamma]$ where

$$\gamma = \frac{2\pi \ln \theta_N}{|\ln \tau|} + \chi, \tag{40}$$

i.e., that the phase varies linearly with the logarithm of the frequency. It is assumed that the reflection coefficient is measured on a transmission line with a characteristic impedance equal to that of the network, i.e., Z_0. In some cases the transmission line impedance Z_t may be different than Z_0. It may be shown that the phase Γ_t of the reflection coefficient when normalized to Z_t is given by

$$\gamma_t = \gamma + 2\tan^{-1}\left[\frac{\left(1 - \frac{Z_0}{Z_t}\right)\tan\frac{\gamma}{2}}{1 + \frac{Z_0}{Z_t}\tan^2\frac{\gamma}{2}}\right]. \tag{41}$$

The last term of (41) represents a periodic deviation of the phase from the desired linear characteristic. The deviation is zero when

$$\tan \frac{\gamma}{2} = 0$$

and maximum when

$$\tan \frac{\gamma}{2} = \pm \left(\frac{Z_t}{Z_0}\right)^{1/2}.$$

The maximum deviation of the phase is given in radians by

$$\Delta_M = 2 \tan^{-1}\left[\sinh \ln \left(\frac{Z_0}{Z_t}\right)^{1/2}\right] \approx \ln \frac{Z_0}{Z_t}. \quad (42)$$

As an example, if $Z_0/Z_t = 1.2$, then $\Delta_M = 10.5°$.

The compensating section of length ψ_0 discussed in Section III introduces a quasi-periodic phase error due to the mismatch between the compensating section of impedance Z_0 and the input characteristic impedance of the truncated network. If it is assumed that this latter impedance is given by $Z_{0,1}$, then the maximum phase error is a function of frequency given by

$$\Delta_M \approx \ln \frac{Z_{0,1}}{Z_0}.$$

It was found that this expression is accurate for the circuit of Fig. 3. The magnitude of Δ_M is approximately proportional to the square of the frequency. An additional phase error, which is proportional to the cube of the frequency, occurs at the higher frequencies because of the nonlinear frequency dependence of the propagation functions of the deleted cells. It is found that the actual electrical length is greater than the assumed ψ_0.

V. Applications

The peculiar frequency dependence of one-port log-periodic circuits is probably useful for only special and limited applications. Radiation Systems Inc. has formed a two-port circuit [13] for which the phase of the transmission coefficient varies linearly with the logarithm of the frequency by terminating two ports of a broadband quadrature hybrid with identical log-periodic circuits like that of Fig. 3. With one of the remaining ports of the hybrid excited, it is found that the signals reflected from the LP circuits appear at the fourth port. This circuit has been used with a four-arm log-spiral direction finding antenna to compensate for the log-periodic rotation of the pattern. An equivalent circuit could be achieved with two LP one-ports and a wide-band magic-T such as the Hughes tapered-line magic-T. In this case one LP circuit would be scaled one half of a period with respect to the other so that their reflection coefficients would be 180° out of phase. This circuit would have the advantage that connector reflections would not distort the phase of the transmission coefficient.

VI. Conclusions

An extensive study has revealed that one-port LP transmission line circuits may be designed such that the phase of the input reflection coefficient varies nearly linearly with respect to the logarithm of the frequency over any desired bandwidth. Phase deviations from linear of a fraction of a degree may be achieved. An empirical but accurate formula for the magnitude of the reflection coefficient was obtained. Magnitudes greater than 0.9 may easily be achieved in practice. Approximate conditions for no end effect were given and the effect of circuit design parameters on the reflection coefficient was determined.

References

[1] R. H. DuHamel and F. R. Ore, "Logarithmically periodic antenna designs," *1958 IRE Nat'l Conv. Rec.*, pt. 1, vol. VI, pp. 139–151.
[2] J. K. Pulfer, "Dispersive properties of broad-band antennas," *Proc. IRE (Correspondence)*, vol. 49, p. 644, March 1961.
[3] R. L. Carrel, "The design of log-periodic dipole antennas," *1961 IRE Internat'l Conv. Rec.*, pt. 1, vol. IX, pp. 61–75.
[4] R. H. DuHamel, "Logarithmically periodic circuits," Research Division, Collins Radio Co., Cedar Rapids, Ia., Tech. Memo., November 1, 1960.
[5] R. Mittra, "Theoretical study of a class of logarithmically periodic circuits," Antenna Lab., University of Illinois, Urbana, Tech. Rept. 59, July 1962.
[6] R. H. DuHamel, "Log-periodic antennas and circuits," in *Electromagnetic Theory and Antennas*. New York: Pergamon, 1963.
[7] R. Mittra and K. E. Jones, "Non-uniform transmission lines with applications to log-periodic antennas," *1964 Proc. NEC*, vol. 20, pp. 23–28.
[8] R. M. Bevensee, "Non-uniform TEM transmission line. Part I —Lossless and log-periodic properties," *Proc. IEE*, vol. 112, pp. 644–654, April 1965.
[9] L. M. Milne-Thompson, *The Calculus of Finite Differences*. London: Macmillan, 1951, Section 138.
[10] G. Boole, *Calculus of Finite Differences*. New York: Dover, 1960, p. 168.
[11] C. C. Montgomery, R. H. Dicke, and E. M. Purcell, *Principles of Microwave Circuits*. New York: McGraw-Hill, 1948, Section 5.23.
[12] E. C. Jordan, *Electromagnetic Waves and Radiating Systems*. New York: Prentice-Hall, 1950, Section 13.02.
[13] J. P. Shelton, private communication.